P.N.Lebedev Physical Institute

High energy and cosmic rays physics

High energy physical department

Preprint N 52

V.M. Alekseyev, S.N. Cherepnya, L.V. Fil'kov and V.L. Kashevarov

Possibility of observation of supernarrow dibaryons with symmetric wave function in $\gamma d \to \pi^{\pm} + \gamma NN$ reactions

Moscow-1996

Abstract

We study the possibility of observation of supernarrow dibaryons with a symmetric wave function in reactions $\gamma d \to \pi^+ + \gamma nn$ and $\gamma d \to \pi^- + \gamma pp$. The method of a dibaryon masses reconstruction over the dibaryon decay products (γnn) and (γpp) is analysed. The Monte-Carlo simulation is used to choose the optimal location of the detectors, to estimate the contribution of the main background processes and to calculate the expected yields of the dibaryon production. It is shown that 100 hours of the exposition time at the microtron MAMI (Mainz) is quite enough to determine whether or not the supernarrow dibaryons with symmetric wave function exist.

1 Introduction

The possibility of existence of many quarks states is predicted by QCD [1]. This is a new kind of the nuclear matter. Of particular interest are narrow six-quark states–dibaryons with decay width of less than a few MeV. The experimental discovery of such states would have important consequences for particle and nuclear physics. An intensive search for narrow dibaryons states has been performed and a number of candidates for this states has been found (see for example [2–12]). Unfortunately, the observed effects are not big and a background is big and uncertain. So it is difficult to claim unequivocally that dibaryon states have actually been found [13]. Therefore, if we want to make unambiguous conclusions about the existance of dibaryons we must regard such type of dibaryons and such processes where the contribution of the dibaryons is very big and a background is small.

We suggest to search dibaryons with symmetric wave function [14–19]. Such dibaryons satisfy the following condition:

$$(-1)^{T+S}P = +1 \tag{1}$$

where T is the isospin, S is the internal spin and P is the dibaryon parity. These are even singlets and odd triplets at $T = 0$, and odd singlets and even triplets at $T = 1$. The decay of the dibaryons with a symmetric wave function into two nucleons is suppressed by the Pauli principle. These dibaryons with the mass $M < 2m_N + m_\pi$ can decay into two nucleons mainly emitting a photon (real or virtual). The contribution of such dibaryons to strong interaction processes of hadrons is very small. However, their contribution to electromagnetic processes on light nuclei may exceed the cross section for the process under study out of the dibaryon resonance by several orders of magnitude [18].

In the frame of the MIT bag model Mulders et al [20] calculated the masses of different dibaryons, in particular, of ones with symmetric wave function. They predicted dibaryons $D(T = 0; J^P = 0^-, 1^-, 2^-; M = 2.11\ GeV)$ and $D(1; 1^-; 2.2\ GeV)$ corresponding to the states $^{13}P_J$ and $^{31}P_1$. However, the obtained dibaryon masses exceed the pion production threshold. Therefore these dibaryons can decay into πNN channel. The possibility of existence of dibaryons with masses $M < 2m + m_\pi$ was discussed by Kondratuk et al [21] in the model of stretched rotating bags with account of spin-orbital quark interaction. In the frame of the chiral soliton model Kopeliovich [22] predicted that the masses of $D(1, 1^+)$ and $D(0, 2^+)$ dibaryons exceed the two nucleon mass by 60 and 90 MeV respectively. These are lower than the pion production threshold.

Unfortunately, all obtained results for the dibaryon masses are very model dependent. Therefore, only experiment could answer the question about the existence of dibaryons with symmetric wave function and their masses.

In the present paper we propose the experiment on the search of the dibaryons with symmetric wave function $D(T = 1, J^P = 1^-, S = 0)$ and $D(1, 1^+, 1)$ in a processes of a

radiative photoproduction of the $\pi^{\pm}$ mesons on the deuteron

$$\gamma d \to \pi^{\pm} D \to \pi^{\pm} + \gamma NN. \tag{2}$$

These dibaryons $D(1,1^+,1)$ and $D(1,1^-,0)$ correspond to states $^{3,3}S_1$ and $^{3,1}P_1$ respectively.

2 The decay widths of the dibaryons $D(1,1^+,1)$ and $D(1,1^-,0)$

The decay widths of the dibaryons under consideration into γNN have been calculated in [18] assuming that they are determined by a diagram in Fig.1 with a singlet virtual level $^{31}S_0$ in the intermediate state. Calculations gave the following expression for the distribution of the probability for the decay $D \to \gamma NN$ over the energy of an emitted photon ω in the dibaryon rest frame

$$\frac{d\Gamma_{D\to\gamma NN}}{d\omega} = \left(\frac{e^2}{4\pi}\right) \frac{\eta_0 g_0^2 f_5^2}{9\pi^2} \frac{\omega_0^2}{M^2} \frac{\sqrt{2(\omega_m-\omega)(M-2\omega)}}{(\omega_0-\omega)^2}\omega. \tag{3}$$

Here $\omega_m = (M^2 - 4m_N^2)/2M$ is the maximum energy of the emitted photon: $\omega_0 = (M^2 - m_0^2)/2M$ is the photon energy corresponding to the singlet virtual state with the mass m_0; η_0 is the probability for the full overlapping of nucleons in the $^{31}S_0$ state. The coupling constant at the vertex $^{31}S_0 \to NN$ is equal to

$$g_0^2 = \frac{8\pi}{m_N|a_s|}$$

where a_s is the singlet length of the NN scattering.

The decay width $\Gamma_{D(1,1^+)\to\gamma NN}$ is obtained by integrating the eq. (2) over ω:

$$\Gamma_{\gamma d\to\pi^0+\gamma pn} = \left(\frac{e^2}{4\pi}\right) \frac{g_0^2}{9\pi^2}\eta_0 f_5^2 \frac{\omega_0^2}{M^2}\sqrt{2M}\left[-3\sqrt{\omega_m} + \frac{\omega_0+2\delta_0}{\sqrt{\delta_0}}\arctan\sqrt{\frac{\omega_m}{\delta_0}}\right] \tag{4}$$

where $\delta_0 = \omega_0 - \omega_m = 2/(Ma_s^2)$. The decay width for the dibaryon $D(1,1^-,0)$ is determined by means of the relation:

$$\frac{4}{f_4^2}\Gamma_{D(1,1^-,0)} = \frac{1}{f_5^2}\Gamma_{D(1,1^+,1)}, \tag{5}$$

the constant $f_{4(5)}^2$ is associated with a change in the dibaryon quantum numbers as a result of the photon emission and a transition to the state $^{31}S_0$.

Table 1 lists the expected decay widths of these dibaryons at various dibaryon masses M [18].

It is evident from eq. (3) that one would expect the appearance of a narrow peak in the distribution of the probability of the decay $D(1,1^{\pm}) \to \gamma NN$ over the photon energy.

$M(GeV)$	1.90	1.93	1.96	1.98	2.00	2.013
$\Gamma_t(1,1^+)$ (eV)	0.2	2.2	8.4	16	26	35
$\Gamma_t(1,1^-)$ (eV)	0.05	0.55	2.1	4	6.5	8.75

Table 1: Decay widths of the dibaryons $D(1,1^+,1)$ and $D(1,1^-,0)$ at various dibaryon masses M. $\Gamma_t \approx \Gamma_{\gamma NN}$.

It is caused by smallness of the value of δ_0. The calculations showed that the interval of photon energies from ω_m to $(\omega_m - 1MeV)$ contains about 70% of the contribution to the decay widths of the dibaryons $D(1,1^{\pm})$. Later at the analysis of the kinematical conditions we will assume that the energy of the emitted photon does not differ from ω_m more than by $2MeV$.

3 The cross sections of the dibaryon $D(1,1^-,0)$ photoproduction

Let us estimate the cross section of the photoproduction of the dibaryon $D(1,1^-,0)$ which, as it is expected, should give the biggest contribution to this process. The gauge invariant amplitude of photoproduction of the dibaryon $D(1,1^-,0)$ may be obtained with help of diagrams in Fig.2. Such dibaryon could be produced only if a pion is emitted from the six quark state of the deuteron. Therefore the vertex of $d \to \pi D$ is written as

$$F_{d\to\pi D(1,1^-,0)} = \frac{g_1}{M}\sqrt{\eta}\Phi_{\mu\nu}G^{\mu\nu}, \tag{6}$$

where $\Phi_{\mu\nu} = r_\mu w_\nu - w_\mu r_\nu$, $G_{\mu\nu} = p_\mu v_\nu - v_\mu p_\nu$, w and v are four-vectors of the dibaryon and deuteron polarization, r and p are the dibaryon and deuteron four-momenta, η is the probability of occurrence of a six-quark state in the deuteron.

It worth noting that for the regarded processes the dibaryon with symmetric wave function may be produced only if the nucleons inside of the deuteron (and $^{31}S_0$ virtual state) are overlapped quite strongly that a six-quark state with the deuteron (virtual singlet state) quantum numbers is formed. Therefore the probabilities of a production and a decay of the dibaryon with symmetric wave function have to be proportional to η and η_0 respectively. According to the estimation of work [23], $\eta = 0.03 - 0.01$. In this paper we assume $\eta = \eta_0 = 0.01$. If in the proposed experiment we do not observe the contribution of the dibaryons larger than 100% of the background one, then, in particular, it may indicate that η (or η_0) is smaller than 0.001.

The following matrix elements correspond to the diagrams in Fig.2a,b,c,d:

$$T_a \;=\; -e\sqrt{\eta}\frac{g_1}{M}\frac{(\epsilon(2p_1+k_1))}{(k_1p_1)}\{(vw)(rP)-(vr)(wP)\}$$

$$
\begin{aligned}
T_b &= e\sqrt{\eta}\frac{g_1}{M}\frac{(\epsilon(2r-k_1))}{(k_1 r)}\left\{(vw)(p_1Q)-(vQ)(p_1w)\right\} \\
T_c &= e\sqrt{\eta}\frac{g_1}{M}\frac{(\epsilon(2q_1+k_1))}{(k_1 q_1)}\left\{(vw)(p_1r)-(vr)(p_1w)\right\} \\
T_d &= T_{d1}+\alpha T_{d2} \\
T_{d1} &= 2e\sqrt{\eta}\frac{g_1}{M}\left\{(vw)(\epsilon r)-(vr)(\epsilon w)\right\} \\
T_{d2} &= 2e\sqrt{\eta}\frac{g_1}{M}\left\{(vw)(\epsilon p_1)-(\epsilon v)(p_1 w)\right\}
\end{aligned}
\tag{7}
$$

where $P=(p_1+k_1)$, $Q=(r-k_1)$; k_1 and q_1 are the four momenta of the photon and the pion; ϵ is a four-vector of the photon polarization; the coefficient α=0,1,2 for production of the π^+, π^0, π^- mesons respectively. The expression for the matrix element T_d is written in the form which ensures the gauge invariance of the amplitude of the dibaryon photoproduction.

The matrix elements (7) are connected with the amplitudes of the dibaryon $D(1,1^-,0)$ photoproduction in different channels as:

$$
\begin{aligned}
T(\gamma d\to\pi^0 D) &= T_a+T_b+T_{d1}+T_{d2} \\
T(\gamma d\to\pi^+ D) &= \sqrt{2}\,(T_a+T_c+T_{d1}) \\
T(\gamma d\to\pi^- D) &= -\sqrt{2}\,(T_a+2T_b-T_c+T_{d1}+T_{d2})
\end{aligned}
\tag{8}
$$

Let us calculate the cross section of the dibaryon $D(1,1^-,0)$ photoproduction in the reactions with formation of π^+ meson. We will use the calibration $\epsilon_0=0$. Then the amplitude $T_a=0$ in lab system $(\epsilon p_1)=0$. As result of calculation for the process $\gamma d\to\pi^+ D$ we have (in lab system):

$$
\begin{aligned}
\frac{d\sigma_{\gamma d\to\pi^+ D}}{d\Omega} = \frac{1}{3}\left(\frac{e^2}{4\pi}\right)\left(\frac{g_1^2}{4\pi}\right)\eta\frac{q^2}{m_d M^2\nu J}\left\{\frac{1}{2m_d^2}[(M^2+m_d^2-t)^2-4m_d^2M^2]+\right. \\
\left. q^2(1-\cos^2\theta_\pi)\left[1+2\frac{(M^2+m_d^2-t)^2+2m_d^2M^2}{(\mu^2-t)^2}-4\frac{M^2+m_d^2-t}{\mu^2-t}\right]\right\}
\end{aligned}
\tag{9}
$$

where

$$
s=2m_d\nu+m_d^2,\quad t=\mu^2-2\nu(q_0-q\cos\theta_\pi),\quad J=q(m_d+\nu)-q_0\nu\cos\theta_\pi,
$$

m_d is the deuteron mass, ν is the incident photon energy, $q_0(q)$ is the π meson energy (momentum). The pion energy q_0 is connected with the pion emission angle θ_π in the following way:

$$
q_0=\frac{1}{c_1}\left[(m_d+\nu)c_2\pm\nu\cos\theta_\pi\sqrt{c_2^2-2\mu^2c_1}\right]
\tag{10}
$$

where

$$
c_1=2[(m_d+\nu)^2-\nu^2\cos^2\theta_\pi],\qquad c_2=s+\mu^2-M^2.
$$

The obtained expression for the cross section of the dibaryon photoproduction in the reaction $\gamma d \to \pi^- D$ is

$$\begin{aligned}\frac{d\sigma_{\gamma d\to\pi^- D}}{d\Omega} &= \frac{1}{3}\left(\frac{e^2}{4\pi}\right)\left(\frac{g_1^2}{4\pi}\right)\eta\frac{q^2}{m_d M^2\nu J}\left\{\frac{1}{2}(M^2+m_d^2-t)^2\left(\frac{1}{m_d^2}+\frac{4}{M^2}\right)-\right.\\ &(M^2+4m_d^2)+q^2(1-\cos^2\theta_\pi)\left[1+\frac{A_1}{(M^2-u)^2}+\frac{A_2}{M^2-u}+\right.\\ &\left.\left.\frac{A_3}{(M^2-u)(\mu^2-t)}+\frac{A_4}{(\mu^2-t)}+\frac{A_5}{\mu^2-t}^2\right]\right\} \qquad (11)\end{aligned}$$

where

$$\begin{aligned}A_1 &= 4\left[(m_d^2-\mu^2+u)^2+4m_d^2u+\right.\\ &\left.\frac{M^2+m_d^2-t}{M^2}\Big((M^2+u)(m_d^2-\mu^2+u)-u(M^2+m^2-t)\Big)\right],\\ A_2 &= 4\left[2(3m_d^2-\mu^2+u)-\frac{1}{M^2}(s-m_d^2)(M^2+m_d^2-t)\right],\\ A_3 &= 8\left[(m_d^2-\mu^2+u)(M^2+m_d^2-t)+m_d^2(M^2+u)\right], \qquad (12)\\ A_4 &= 4(M^2+3m_d^2-t),\\ A_5 &= 2[(M^2+m_d^2-t)^2+2m_d^2M^2].\end{aligned}$$

Here $u=(p_1-q_1)^2=m_d^2+\mu^2-2m_dq_0$.

In the numerical calculations we assumed that $\eta=\eta_0=0.01$. The coupling constant $g_1^2/4\pi$ is unknown. This is the coupling constant of the strong interaction. Not to overestimate the value of the cross section we took it equal to 1. To estimate the dibaryon contribution at different masses M we will assume the possibility of existance of the dibaryons with masses M=1.9, 1.95 and 2.00 GeV. Results of the calculations of the differential and total cross sections of the dibaryon $D(1,1^-0)$ production in the reactions $\gamma d \to \pi^+ D$ and $\gamma d \to \pi^- D$ are presented in Fig.3 and 4, respectively. The main contribution to these processes are given by the diagram in Fig.2c.

Let us consider to carry out a search of the dibaryons at the tagged photon beam of the microtron MAMI.

4 Analysis of the dibaryon $D(1,1^-,0)$ production in the reaction $\gamma d \to \pi^+ + \gamma nn$

Taking into account a high energy resolution of the tagging system ($\Delta\nu_1 = 2MeV$), an optimal method of the dibaryon identification could be the missing mass one. It would allow, at an additional detection of the final photon, to separate reliably from a background.

However in this case a magnetic spectrometer with high resolution is necessary to detect charged pions with the kinetic energy 100–600MeV.

Another way to recognize the dibaryon is a reconstruction of the dibaryon mass by detecting the decay products. The information about the tagged photon energy could be used to suppress background processes. This method of dibaryon identification is studied in the present paper in detail.

The Monte-Carlo simulation was used to generate events of the dibaryon production in the processes (2) and obtain background reactions

$$\gamma d \to \pi^{\pm} + \pi^0 + NN, \tag{13}$$

$$\gamma d \to \pi^{\pm} + \gamma + NN. \tag{14}$$

For simulation of dibaryon photoproduction we used the expression (9) and (11) for the differential cross sections. Studying the reactions (13) we used the values of the total cross sections for the reactions $\gamma p \to \pi^+\pi^0 n$ [25]. The total cross section for the reaction (14) in an energy region $\nu_1 = 500 - 800MeV$ was took equal to $0.01(\mu b)$, which is a wittily abnormally high value.

Let us consider in the first a dibaryon production in the reaction

$$\gamma d \to \pi^+ D \to \pi^+ + \gamma nn. \tag{15}$$

In this case we must detect the photon and two neutrons.

In order to find the optimal location of the setup, an analysis of distributions of kinematical variables for investigating reactions was carried out. These distributions are presented in Fig.5–10 for the dibaryon masses 1900, 1950 and 2000 MeV. Fig.5 shows the distributions over the energy and the emission angle of the neutrons from the dibaryon decay. The distributions over $\cos\theta_n$ in this figure corresponds to an interval of the neutron energy from 10 to 100MeV. The average angle of the neutron detector location is choose from these distributions to be equal to 45°. The choice of this angle in the side of bigger dibaryon mass is caused by the bigger cross section of the production of the dibaryon with smaller mass.

Fig.6 demonstrates distributions over the energy of the photon from the dibaryon decay and over $\cos\theta_{\gamma n}$, where $\theta_{\gamma n}$ is an angle between the neutron and the final photon. These distributions were obtained also for the neutron energy in the interval 10–100MeV. It is evident from these distributions that the optimal angle of the γ detector location depends on the dibaryon mass. For $M = 1900MeV$ this angle coincides with the angle of the location of the neutron detector. For $M = 2000MeV$ the optimal location of the γ detector is opposite to the neutron detector. Taking into account increase of the cross section at decrease of the dibaryon mass we chose the latter position of the γ detector ($\theta_\gamma = 135°$).

As the neutron detector we shall consider the time-of-flight scintillator detector consisted of 5 planes with sizes $300 \times 300 \times 5\ cm^3$. Each plane contains from 15 scintillator counters with sizes $300 \times 20 \times 5\ cm^3$. This detector has a neutron detection efficiency 20–30% in the energy interval 10–100MeV.

detectors	θ	φ	$R(cm)$	sizes (cm^2)
γ (BaF_2)	235°	270°	100	$40 \times 50 \times 25$ (segmented – 64)
n (TOF)	45°	90°	400	$300 \times 300 \times 5$ (5 planes)

Table 2: Parameters and location of the γ and neutron detectors.

$M\ (MeV)$	$\varepsilon\ (\%)$
1900	0.05
1950	0.09
2000	0.16

Table 3: Geometrical efficiency of the setup at different values of M.

As a γ detector we shall assume the block from 64 BaF_2 crystal with sizes $40 \times 50 \times 24\ cm^3$. The parameters of the setup and the location of the γ and neutron detectors are listed in Table 2.

It was simulated quantity of events for the processes (2), (13) and (14) corresponding to 1 hour of the exposition time of the microtron MAMI for the energy interval of the tagged photons 500–$800MeV$, the incident photon intensity $1.3 \cdot 10^6 sec^{-1}$ at $\nu_1 = 500MeV$ in the interval $\Delta\nu_1 = 2MeV$ and a thickness of the deuteron target $10cm$. Obtained a geometrical efficiency at the different values of the dibaryon mass are presented in Table 3.

Increase of the geometrical efficiency of the setup for the dibaryon with bigger mass is well founded as increase of the dibaryon mass results in growth of dibaryon identification errors and the contribution of the background processes.

Let us consider kinematical parameters of two neutrons from the dibaryon decay. The kinetic energy of these neutrons in cms are close to zero (0.07–1.9 MeV for $M = 1900 - 2000\ MeV$). In lab.syst. the emission angles and the energies of neutrons are determined mainly by motion of the cms. Both neutrons in lab.syst. have the close emission angles. Fig.7b,e,h show the distributions over $\cos\theta_{nn}$, where θ_{nn} is the angle between the emission directions of these neutrons. It is evident that $\theta_{nn} \leq 15^\circ$.

The average neutron emission angle in lab.syst. coincides practically with the emission angle of the dibaryon. In this case the photons, emitted to the opposite direction, have minimum values of the energy (the energy spectra for such photons are shown in Fig.7a,d,g) and so minimum values of the absolute error of this energy measurement.

In Fig.7c,f,i the distributions over $\delta T_{nn} = 2|T_{n1} - T_{n2}|/(T_{n1} + T_{n2})$ are presented. These distributions show that the energies of two neutrons differ by smaller than 50%. To detect such pairs of neutrons, high enough discretness of the neutron detector is necessary.

The carried out simulation resulted in the expected yields of the reactions (13)–(15) for 1 hour of the exposition time of the microtron MAMI for described setup (Table 4). The first line of Table 4 shows the total numbers of the events. The following lines demonstrate numbers of events left after using limitation of the value of the neutron energy, two neutron

	M=1.9GeV	M=1.95GeV	M=2.00GeV	background
simulated events	421400	348200	277800	17897900
T_n=10-100MeV	229400	200700	181800	5010700
nn	25700	27100	23100	108900
γnn	202	307	444	736
M=1870-2040MeV	202	307	444	636

Table 4: The expected yields of the dibaryon production in the process $\gamma d \to \pi^+ + D \to \pi^+ + \gamma nn$ and the background reactions (13) and (14) for 1 hour of exposition time of the microtron MAMI.

coincidence condition, triple coincidences γnn and limited range of the dibaryon masses.

The yields of the dibaryon production are expected to be 200–400(1/hour) for the dibaryon masses in the interval $M = 1900 - 2000 MeV$. If take into account that the efficiency of detection of two neutrons by the neutron detector is about 0.05%, then to obtain such yields really it is necessary to have 20 hours of the exposition time. The expected spectra of the dibaryon mass for M=1900, 1950, 2000 MeV are shown in the Fig.8a (without background) and Fig.8b (with the background from the reactions (13) and (14)).

We did not take into consideration the background from random coincidences and from the reaction

$$\gamma + d \to \pi^0 np \tag{16}$$

In principle, the detection of the neutron from this reaction in two blocks of TOF detector could imitate the detection of two neutrons. Besides, it is possible to detect a photon from the π^0 meson decay. The contribution of this background should be considered. However, preliminary estimations indicate that this contribution does not exceed one from the process (13).

Taking into account all mentioned above, it needs about 100 hours of exposition time to obtain unambiguous result.

5 Analysis of the dibaryon $D(1, 1^-, 0)$ production in the reaction $\gamma d \to \pi^- + \gamma pp$

The analogous simulations were carried out for the process

$$\gamma + d \to \pi^- + D \to \pi^- + \gamma pp \tag{17}$$

In this case we must detect the photon and two protons. To detect the photon it is assumed to use the γ detector such as above. To detect the protons it could be used a time-of-flight scintillator spectrometer consisted of 3 planes with sizes $300 \times 300 \times 5 cm^3$. Each plane contains 15 scintillator blocks with sizes $300 \times 20 \times 5 cm^3$. To limit a range of charged

particles, this spectrometer should be supplemented by a plane of the anticoincident counters behind of the TOF detector.

In order to identify the protons the relation of range–energy and the time of flight of the detected particle will be used.

Results of the kinematical investigation for the reaction (17) are presented in Fig.9–11. Fig.9a,c,e show that the proton energy does not exceed $150MeV$. The range of a proton with such an energy corresponds to the thickness of the considering spectrometer ($15cm$). This spectrometer allows to detect protons with the energy higher than $\sim 50MeV$. Protons with lower energy either are absorbed or are strongly scattered in the target and air.

The angular distributions of the protons with energy 50–$150MeV$ are shown in Fig.9b,d,f. These distributions give the average angle of the proton detector location equal to 35°.

Fig.10 demonstrates the energy and angular distributions of the photons from the reaction (17) when the protons have energy in the region of 50–$150MeV$. Using the same arguments as in the previous case we chose the angle of the γ detector location 145°.

Fig.11 shows the distributions over the photon energy, the angle between two protons θ_{pp} and $\delta T_{pp} = |T_{p1} - T_{p2}|/(T_{p1} + T_{p2})$ for different dibaryon masses at the chosen location of the detectors. Fig.11a,d,g indicate (see also Fig.7a,d,g) that the narrow peak in the photon spectrum can be an additional signal of the dibaryon production.

The expected yields of the dibaryon production in the reaction (17) are equal to $\sim$ 150/hour for each dibaryon mass. The expected spectra of mass for three dibaryon masses are presented in Fig.12a (without background) and Fig.12b (with the background).

The main difficulty of investigation of the reaction (17) is identification and determination of energy of two protons flying at close angles. It can decrease the efficiency of the setup and make worse the resolution over mass. Moreover it is necessary to consider the random background contribution. All these could lead to increase of the exposition time.

We propose to investigate the process (17) simultaneously with the process (15), where it is necessary to have $\sim$ 100 hours of the exposition time. This time would be quite enough for research of the process (17) too. The proposed location of the setup in this case is shown in Fig.13. Investigation both of these reactions allows answer a question about existance of the dibaryons with symmetric wave function more unambiguously and to decrease the systematic experimental errors.

6 Conclusion

We studied the possibility of observation of the supernarrow dibaryons with the symmetric wave function in the reactions of charged pion photoproduction. The method of the dibaryon identification by detecting the dibaryon decay products was analyzed in detail. The cross sections of the dibaryon photoproduction were calculated. To find the optimal location of the detectors the kinematical analysis was used. The contributions of the main background processes were estimated and the expected yields of the dibaryon production

were calculated. The calculations showed that 100 hours of the exposition time of the microtron MAMI (Mainz) would be quite enough to determine whether or not the supernarrow dibaryons with the symmetric wave function exist. It was indicated that the additional signal of the dibaryon production can be the narrow peak in the photon spectrum.

If in this experiment we does not observe the contribution of the dibaryons larger than 100% of the background one, then, in particular, it may indicate that the probability of six-quark state inside of the deuteron (or $^{31}S_0$ state) is smaller than 0.001.

The suggested search of the dibaryon production in the both (15) and (17) reactions simultaneously would allow to make more correct conclusion about such dibaryons existance and decrease the systematical experimental errors.

Acknowledgments

We thank J.Ahrens, D,Drechel, J.Friedrich, N.Nikolaev and Th.Walcher for stimulating discussion. This work was supported in part by the Russian Fund for Fundamental Research (Project number: 96-02-16530-A).

References

1. R.L. Jaffe, Phys.Rev.Lett. **38** (1977) 195; P.J.G. Mulders, A.T. Aerts and J.J. de Swart, Phys.Rev.Lett. **40** (1978) 1543, Phys.Rev. **D21** (1980) 2653; D.B. Lichtenberg *et al.*, Phys.Rev. **D18** (1978) 2569; V. Matveev and P. Sorba, Lett.Nuovo Cim. **20** (1977) 425.

2. A.A. Bairamov *et al.*, Sov.J.Nucl.Phys. **39** (1984) 26.

3. S.A. Azimov *et al.*, Sov.J.Nucl.Phys. **42** (1985) 579.

4. O.B. Abdinov *et al.*, Sov.J.Nucl,Phys. **44** (1986) 978.

5. B. Bock *et al.*, Nucl.Phys. **A459** (1986) 573.

6. O.B. Abdinov *et al.*, JINR preprint PI-88-102.

7. B. Tatischeff *et al.*, Z.Phys. **A328** (1987) 147.

8. V.P. Andreev *et al.*, Z.Phys. **A327** (1987) 363.

9. B. Tatischeff *et al.*, Relativistic Nuclear Physics and Quantum Chromodynamics (Proc. of the IX Intern. Seminar on High Energy Physics Problems, Dubna, Russia, 1988), Dubna, JINR, (1988), p.317.

10. Yu.A Troyan, *et al.*, Sov.J.Nucl.Phys. **54,** (1991) 1301.

11. V.V. Glagolev *et al.*, JINR preprint EI-89-246.

12. E.N. Komarov, Relativistic Nuclear Physics and Quantum Chromodynamics (Proc. of the XI Intern. Seminar on High Energy Physics Problems, Dubna, Russia, 1994), Dubna, JINR, (1994), p.321.

13. K.K. Seth, Int. Conf. on medium and high energy physics, Taipei, Taiwan, 1988.

14. L.V. Fil'kov, Sov.Physics—Lebedev Inst. Reports No. 11 (1986) 49.

15. L.V. Fil'kov, Sov.J.Nucl.Phys. **47** (1988) 437.

16. D.M. Akhmedov *et al.*, Proceed. of the 8th Seminar "Electromagnetic interactions of nuclei at low and medium energies", Moscow, (1991), p.228.

17. D.M. Akhmedov *et al., ibid*, p.252.

18. D.M. Akhmedov and L.V. Fil'kov, Nucl.Phys. **A544** (1992) 692.

19. S.B. Gerasimov and A.S. Khrykin, JINR Rapid Communication No. 61571-92.

20. P.J.G. Mulders *et al.*, Phys. Rev. D **19** (1979) 2635.

21. L.A. Kondratuk *et al.*, Sov.J.Nucl.Phys. **45,** (1987) 1252.

22. V.B. Kopeliovich, Sov.J.Nucl.Phys. **58,** (1995) 1317.

23. L.A. Kondratyuk *et al.*, Yad.Fiz. **43** (1986) 1396.

24. M. Anghinolfi *et al.*, Research Summaries of the Gordon Conference 1994 on Photo-Nuclear Physics, p.149.

25. M. Maccormick *et al.* (DAPHNE collaboration), Phys.Rev. C, to be published.

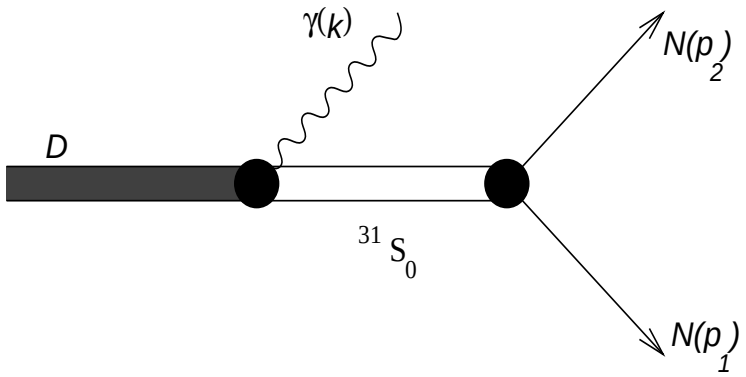

Figure 1: The diagram of the dibaryon decay into γNN.

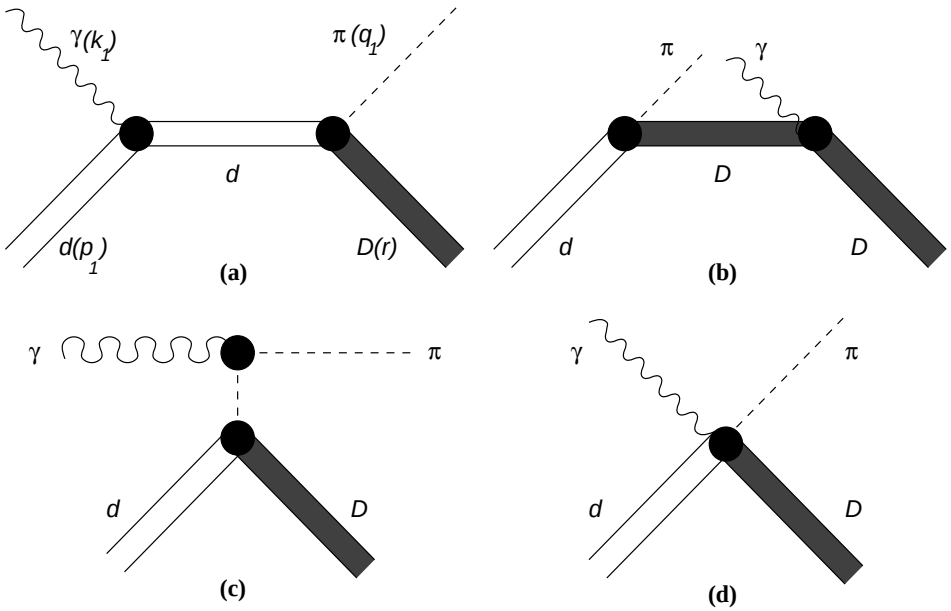

Figure 2: The diagrams of the dibaryon production in the process $\gamma d \to \pi D$.

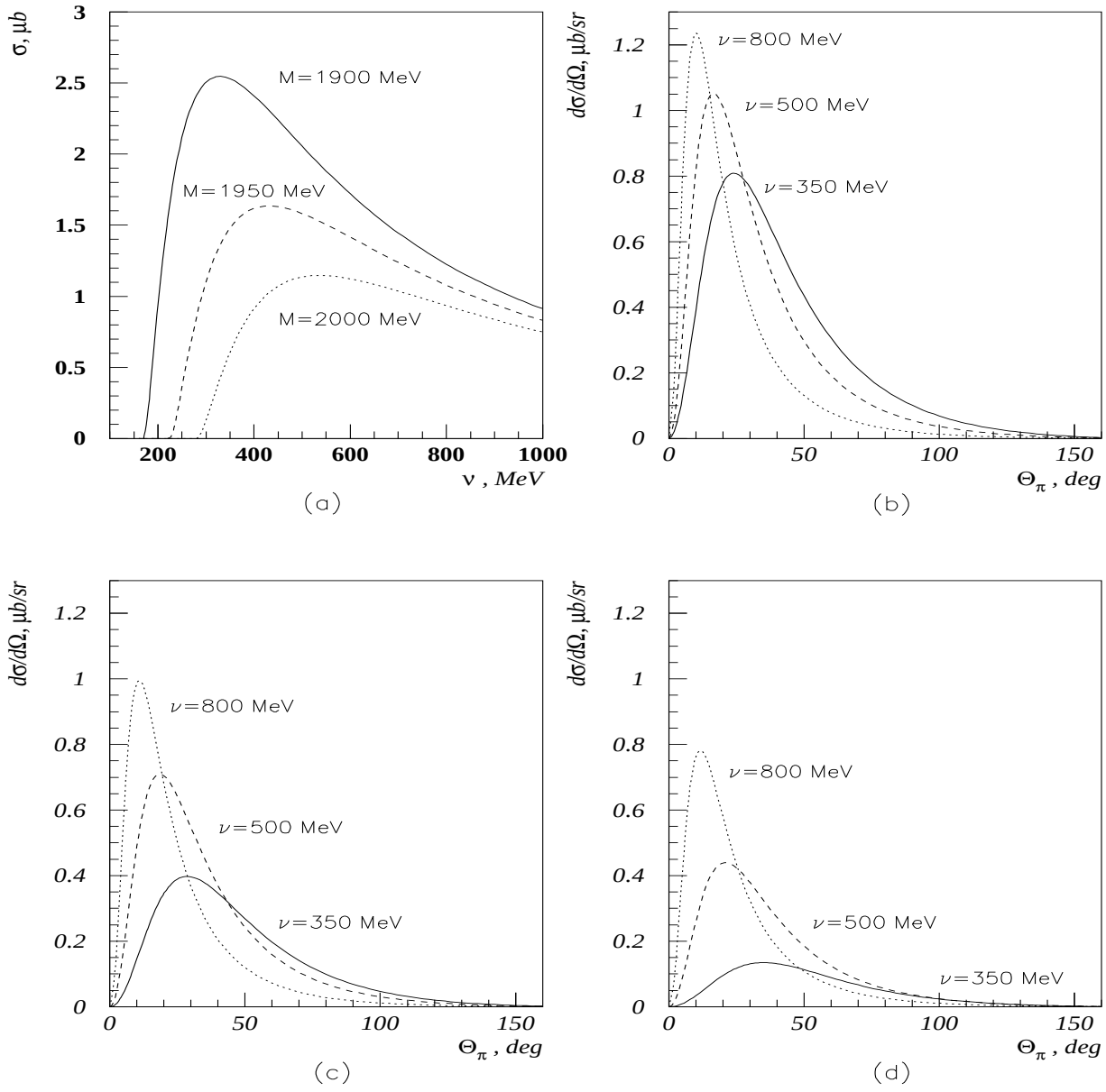

Figure 3: The cross sections of the dibaryon $D(1, 1^-, 0)$ production in the reaction $\gamma d \to \pi^+ D$ for the different dibaryon masses; a)–the total cross sections; b,c,d)–the differential cross sections for M=1900, 1950 and 2000 MeV consecutively.

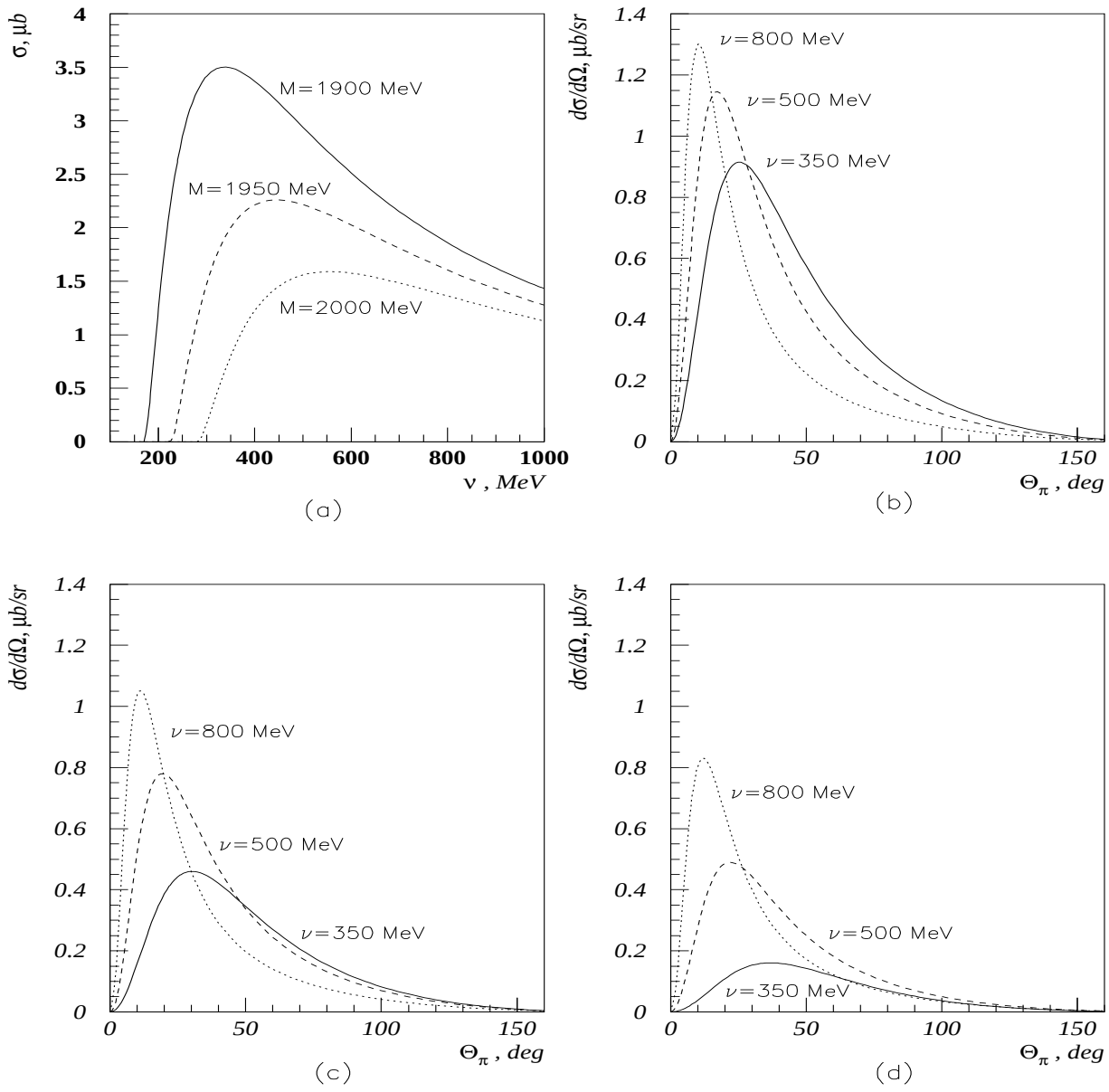

Figure 4: The cross sections of the dibaryon $D(1, 1^-, 0)$ production in the reaction $\gamma d \to \pi^- D$; a)–the total cross sections; b,c,d)–the differential cross sections for M=1900, 1950 and 2000 MeV consecutively.

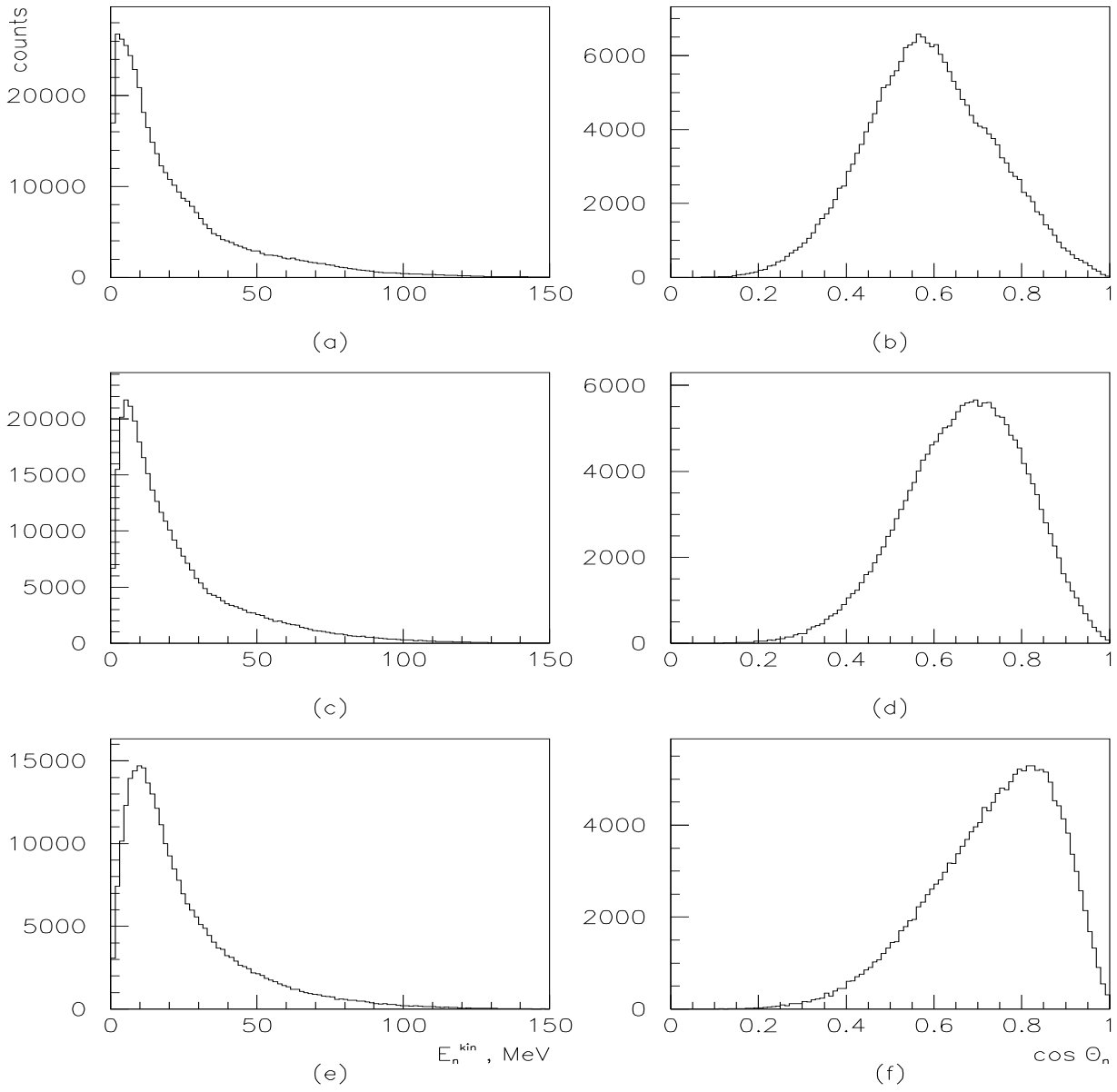

Figure 5: The energy (a,c,e) and angular (b,d,f) distributions of the neutrons from the decays of the dibaryons with different masses: a,b)- M=1900 MeV, c,d)- M=1950 MeV and e,f)- M=2000 MeV.

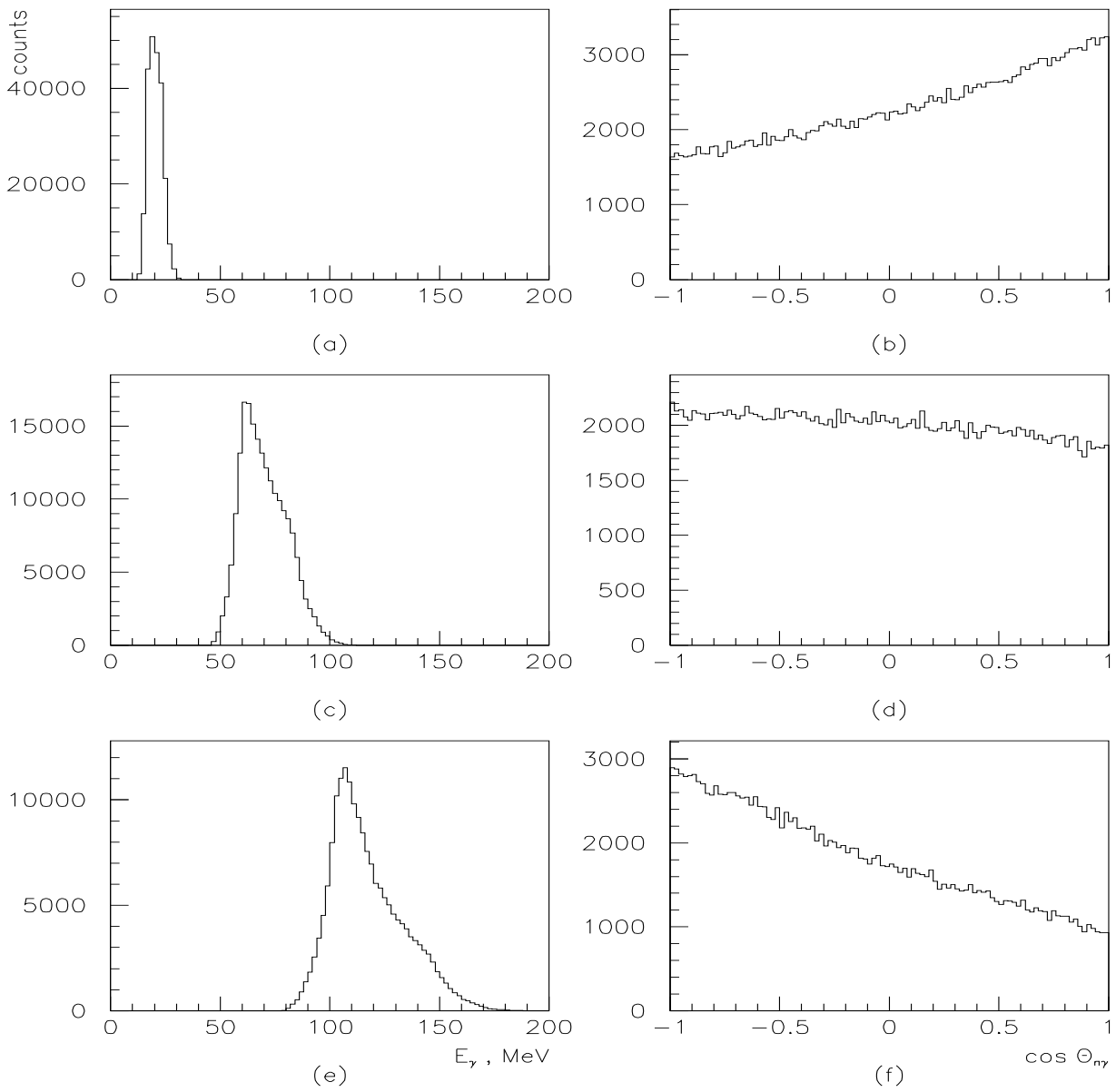

Figure 6: The energy (a,c,e) and angular (b,d,f) distributions of the photons from the decays of the dibaryons produced in the reaction $\gamma d \to \pi^+ D$ with different masses: a,b)- M=1900 MeV, c,d)- M=1950 MeV and e,f)- M=2000 MeV.

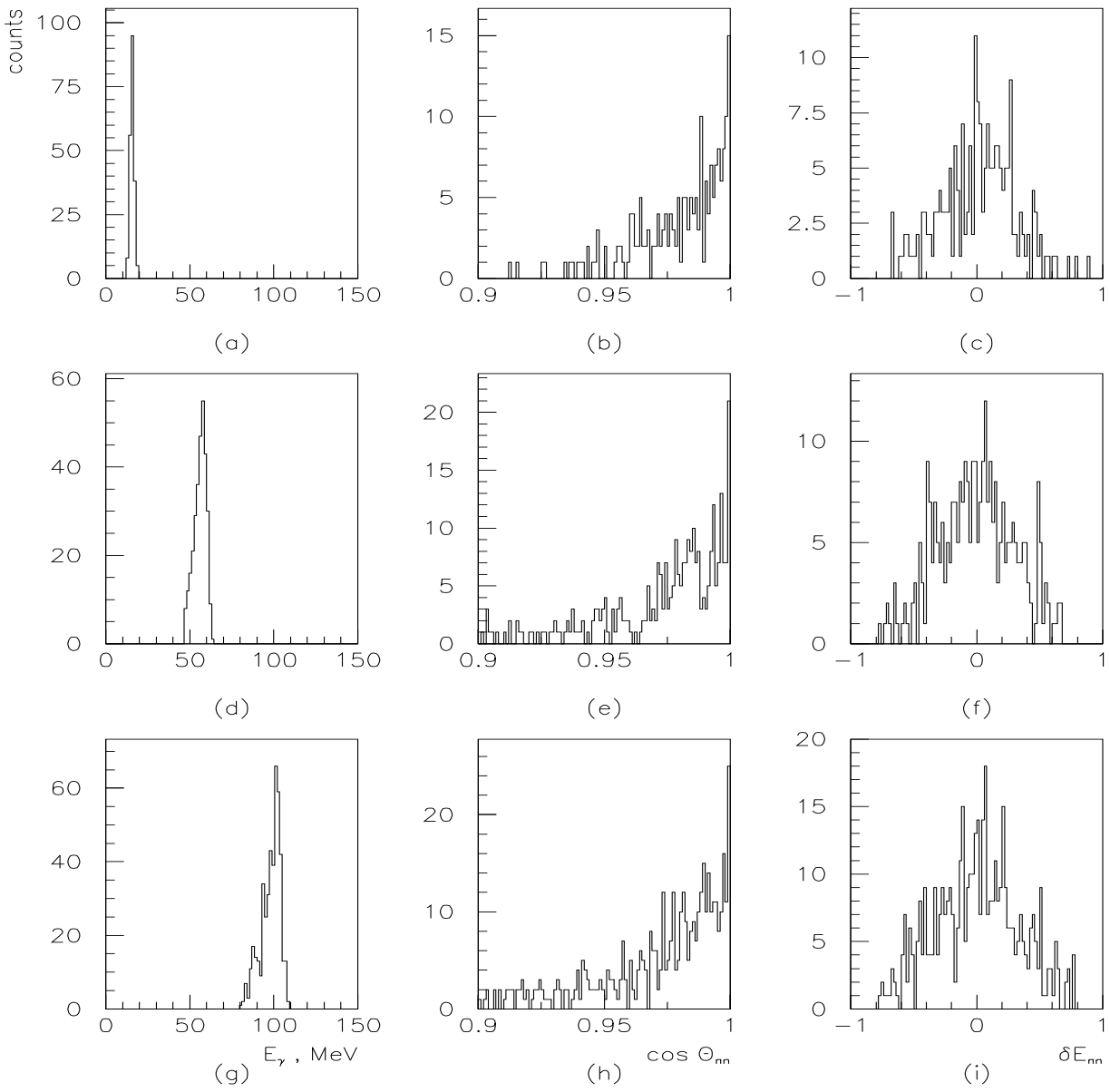

Figure 7: a,d,g)– energy spectra of the photons detected by the setup at the triple coincidences condition (γnn); b,e,h)– the distributions over $\cos\theta_{nn}$; c,f,i)– the distributions over δT_{nn} for different masses: a,b,c)- M=1900 MeV, d,e,f)- M=1950 MeV and g,h,i)- M=2000 MeV.

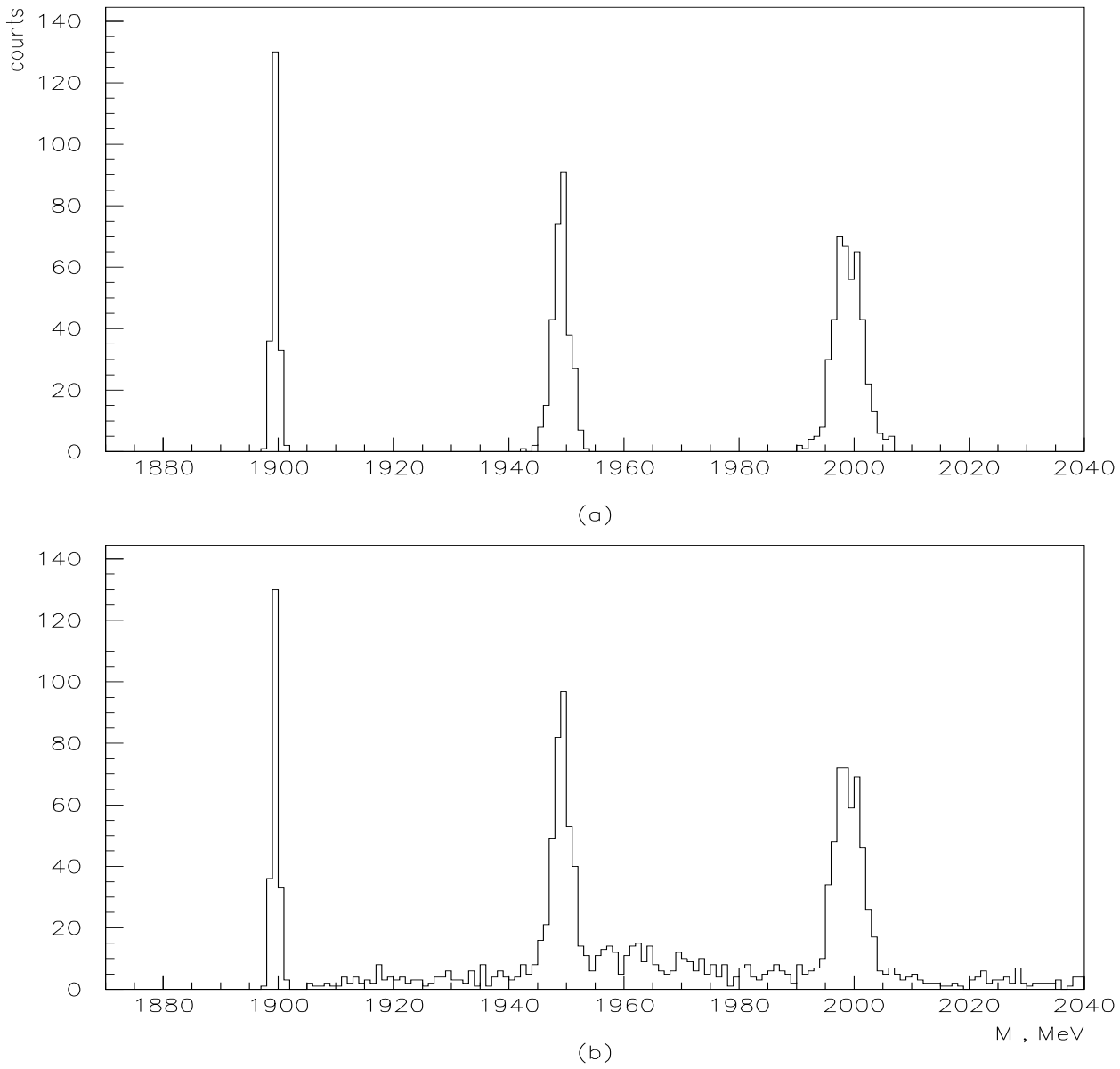

Figure 8: The expected spectra of mass of the dibaryons produced in the reaction $\gamma d \to \pi^+ D$ with the masses M=1900, 1950 and 2000 MeV; a)– without background contribution; b)– with the contribution of the background from the processes (13) and (14).

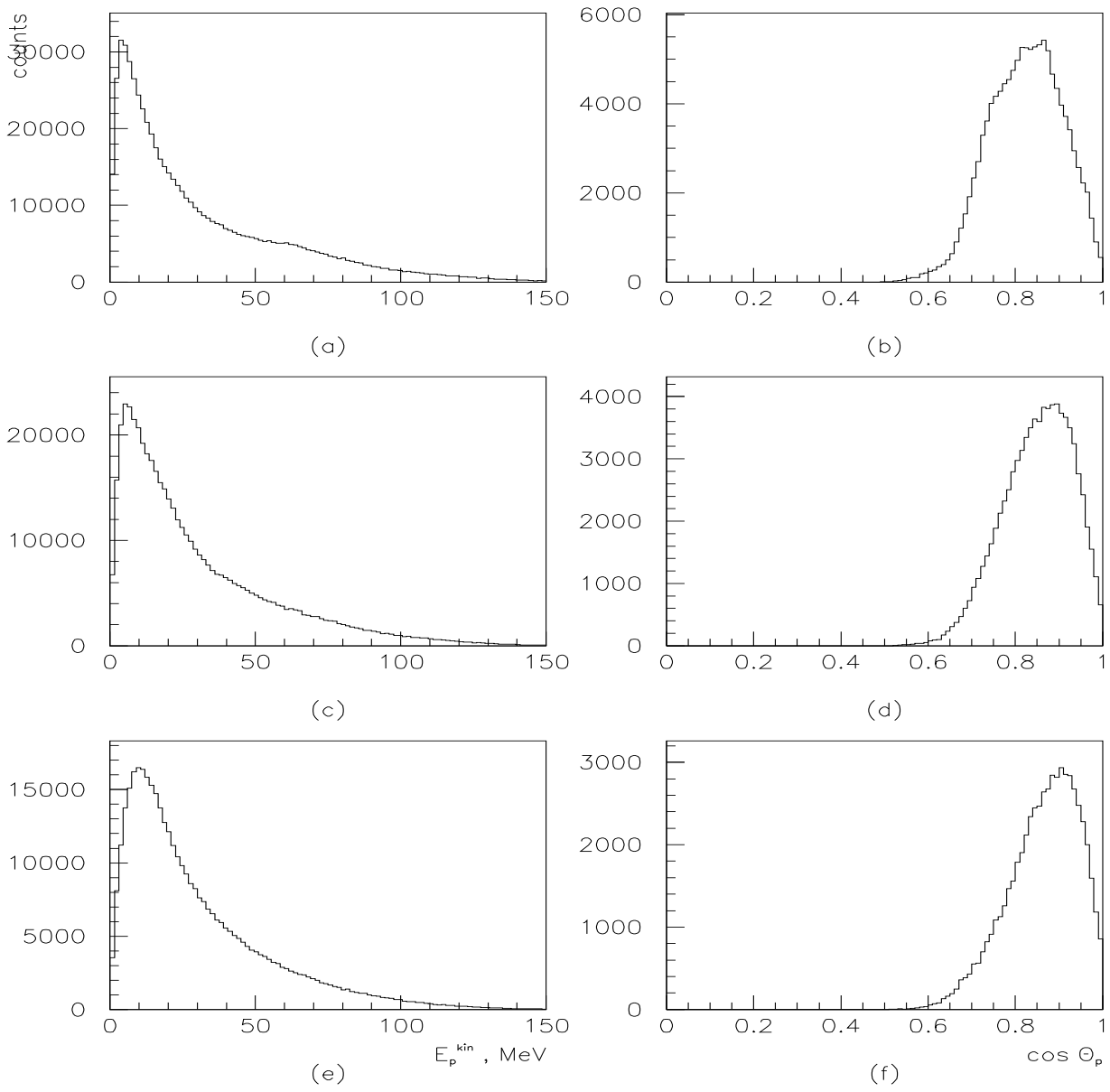

Figure 9: The energy (a,c,e) and angular (b,d,f) distributions of the protons from the decays of the dibaryons with different masses: a,b)- M=1900 MeV, c,d)- M=1950 MeV and e,f)- M=2000 MeV.

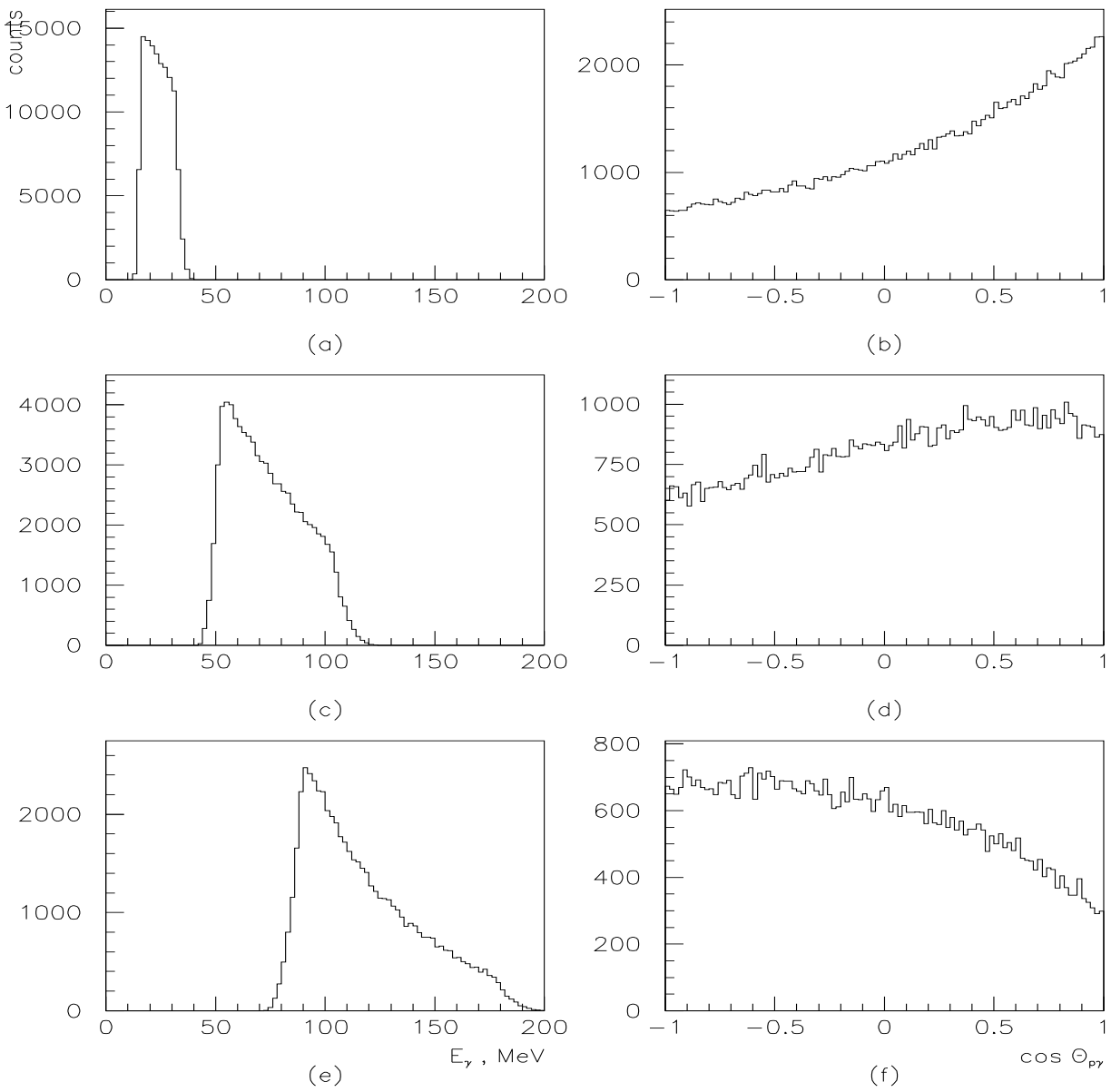

Figure 10: The energy (a,c,e) and angular (b,d,f) distributions of the photons from the decays of the dibaryons produced in the reaction $\gamma d \to \pi^- D$ with different masses: a,b)- M=1900 MeV, c,d)- M=1950 MeV and e,f)- M=2000 MeV.

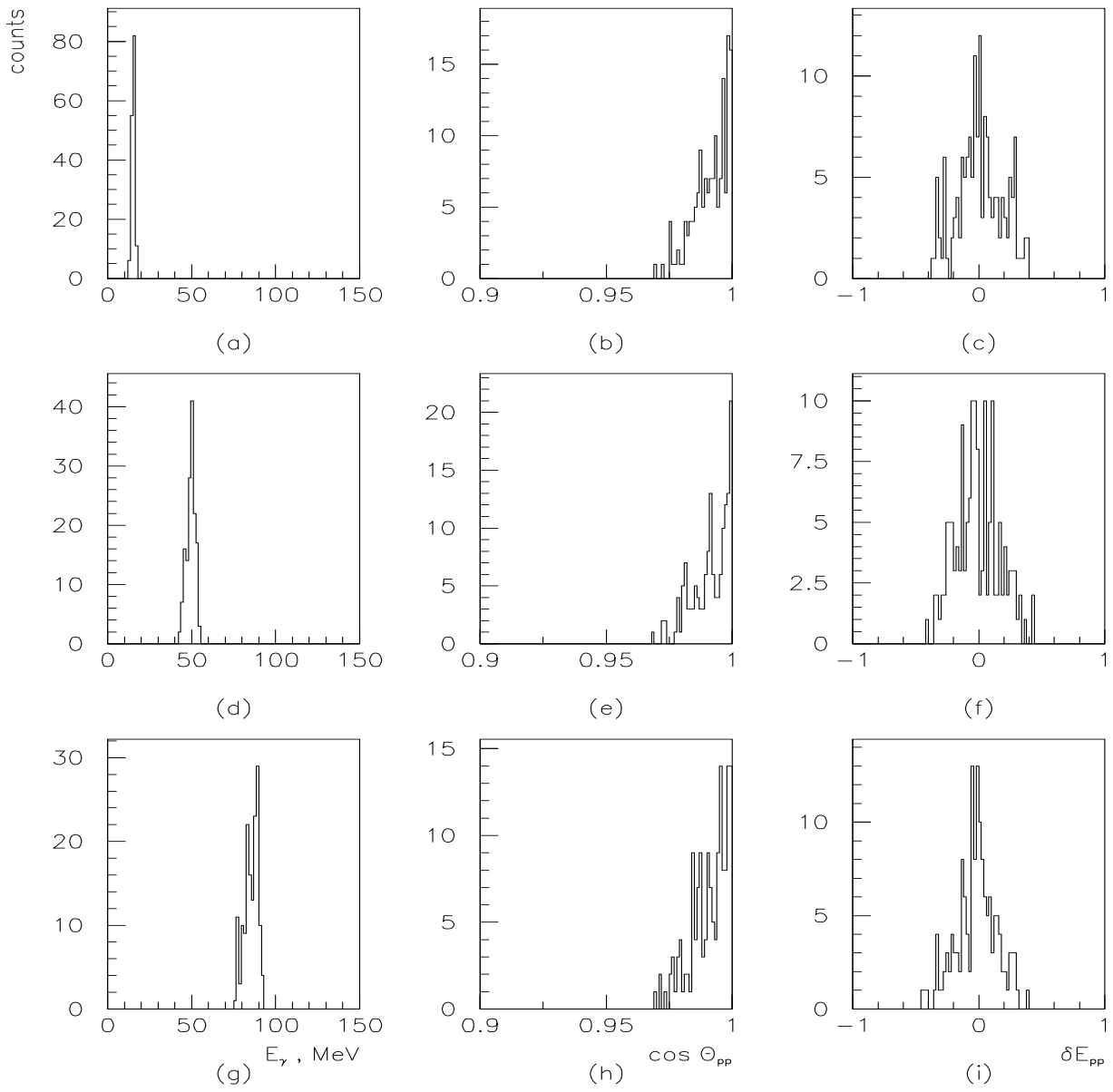

Figure 11: a,d,g)– energy spectra of the photons detected by the setup at the triple coincidences conditions (γpp); b,e,h)–the distributions over $\cos\theta_{pp}$; c,f,i)– the distributions over δT_{pp} for different masses: a,b,c)- M=1900 MeV, d,e,f)- M=1950 MeV and g,h,i)- M=2000 MeV.

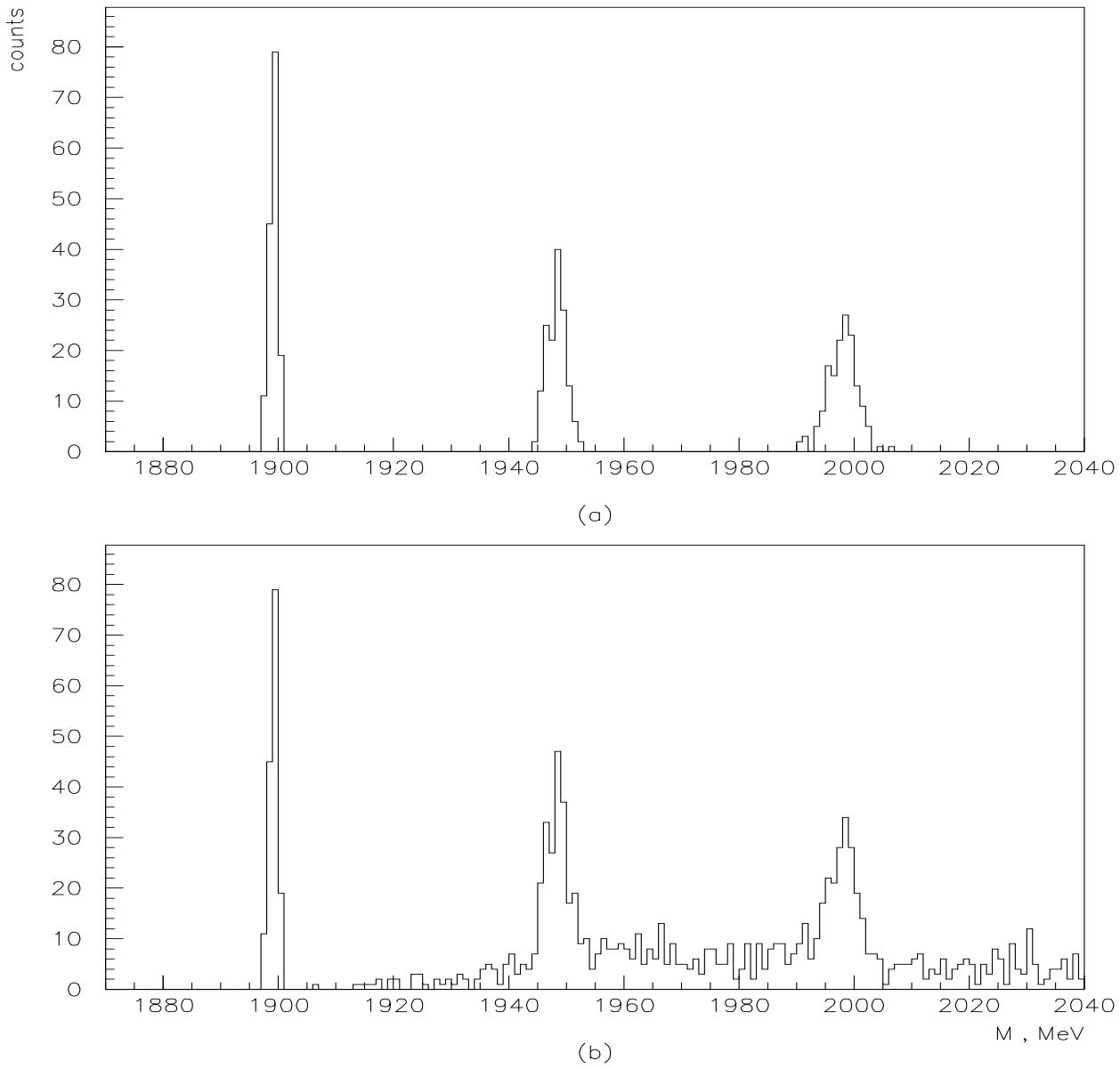

Figure 12: The expected spectra of mass of the dibaryons produced in the reaction $\gamma d \to \pi^- D$ with the masses M=1900, 1950 and 2000 MeV; a)– without background contribution; b)– with the contribution of the background from the processes (13) and (14).

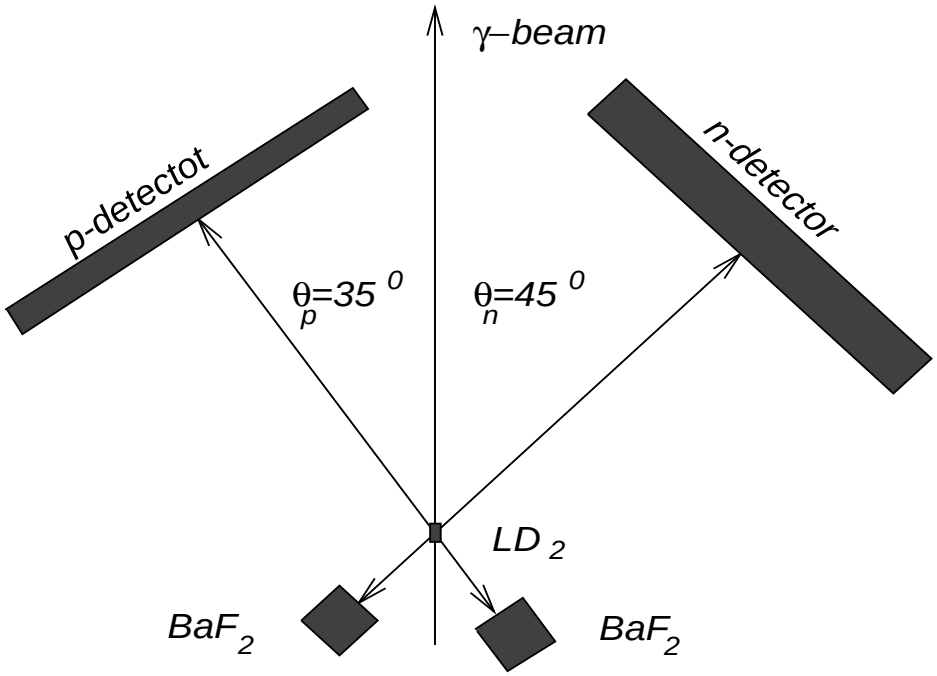

	R(cm)	detector sizes(cm)	block sizes(cm)	number of blocks
n-detector	400	300x300x25	300x20x5	75
p-detector	400	300x300x15	300x20x5	45
BaF_2	100	40x50x25	Ø6x25	64

Figure 13: Location of the detectors.